

Antitumor effects and mechanisms of 1,25(OH)₂D₃ in the Pfeiffer diffuse large B lymphoma cell line

JING HAN^{1,2}, YONGHONG TANG², MEIZUO ZHONG² and WENLIN WU³

¹Department of Oncology, Tongji Hospital, Tongji Medical College, Huazhong University of Science and Technology, Wuhan, Hubei 430030; ²Department of Oncology, Xiangya Hospital, Central South University, Changsha, Hunan 410011; ³Department of Pediatrics, Guangzhou Women and Children's Medical Center, Guangzhou Medical University, Guangzhou, Guangdong 510000, P.R. China

Received October 8, 2018; Accepted August 6, 2019

DOI: 10.3892/mmr.2019.10756

Abstract. Diffuse large B cell lymphoma (DLBCL) represents the most common subtype of non-Hodgkin lymphoma in China. 1,25-Dihydroxyvitamin D₃ [1,25(OH)₂D₃] has been shown to possess significant antitumor potential and is degraded by 25-hydroxyvitamin D-24-hydroxylase (CYP24A1). In the present study, the role of CYP24A1 and autophagy, and their underlying mechanisms in the anticancer effects of 1,25(OH)₂D₃ in DLBCL cells, were investigated. It was found that the levels of CYP24A1 in DLBCL lymph node tissues were higher than in hyperplasia lymphadenitis tissue. Moreover, the expression of CYP24A1 was positively associated with the Ann Arbor stage and the International Prognostic Index in patients with DLBCL, and negatively associated with the clinical response to treatment. Patients >60 years of age were found to have a higher level of CYP24A1. 1,25(OH)₂D₃ inhibited the proliferation of the Pfeiffer DLBCL cell line and increased the G1 phase population of Pfeiffer cells. Rapamycin (RAPA) in combination with 1,25(OH)₂D₃ increased the G1 phase distribution of Pfeiffer cells. Furthermore, RAPA blocked

the increase of CYP24A1 and vitamin D receptor (VDR) expression induced by 1,25(OH)₂D₃. 1,25(OH)₂D₃ induced the formation of autophagosomes, increased the expression of autophagy related protein light chain (LC)3II/LC3I and reduced the expression of the ubiquitin binding protein P62. In addition, 1,25(OH)₂D₃ decreased the phosphorylation of AKT and mammalian target of RAPA (mTOR), and downstream targets eukaryotic translation initiation factor 4E-binding protein 1 and ribosomal protein S6 kinase β-1 in Pfeiffer cells. The results from the present study suggested that CYP24A1 may be a novel prognostic indicator for DLBCL. 1,25(OH)₂D₃ inhibited proliferation and induced autophagy of Pfeiffer cells. In addition, 1,25(OH)₂D₃ increased the G1 phase population of Pfeiffer cells. These effects may be mediated by inhibition of the AKT/mTOR/PI3K signaling pathway. RAPA increased the cell cycle arrest induced by 1,25(OH)₂D₃ by blocking the upregulated expression of CYP24A1 and VDR.

Introduction

Diffuse large B cell lymphoma (DLBCL) represents the most common subtype of non-Hodgkin lymphoma (1) and accounts for ~40% of newly diagnosed cases of non-Hodgkin lymphoma annually in China (2). DLBCL is an aggressive form of lymphoma, with a highly variable clinical manifestation, histology, outcome and prognosis (1). Despite the fact that patients with DLBCL who receive comprehensive treatment, including radiotherapy, chemotherapy and combined therapy with molecular targeted therapy, have a high chance of achieving partial or complete remission, some patients are resistant to first line therapy or relapse, leading to reduced survival rates, psychological and physical pain (1). Furthermore, the medical cost of DLBCL is high (1). Therefore, identifying new strategies for the treatment of DLBCL is needed.

B lymphocyte receptor (BCR) signaling is important for B cell lymphoma proliferation (3). BCR signaling can activate the PI3K signaling pathway, leading to the production of phosphatidylinositol 3,4,5-triphosphate, which initiates a large number of signaling cascades, including those involving serine/threonine kinase AKT (4). This can lead to uncontrolled growth by inhibiting the function of the cell cycle inhibitors p21 and

Correspondence to: Professor Meizuo Zhong, Department of Oncology, Xiangya Hospital, Central South University, 88 Xiangya Road, Changsha, Hunan 410011, P.R. China
E-mail: zhongmeizuo_csu@csu.edu.cn

Dr Wenlin Wu, Department of Pediatrics, Guangzhou Women and Children's Medical Center, Guangzhou Medical University, 9 Jinsui Road, Tianhe, Guangzhou, Guangdong 510000, P.R. China
E-mail: wenlinwu@csu.edu.cn

Abbreviations: 1,25(OH)₂D₃, 1,25-dihydroxyvitamin D₃; 4EBP, eukaryotic translation initiation factor 4E-binding protein 1; CYP24A1, 25-hydroxyvitamin D-24-hydroxylase; DLBCL, diffuse large B cell lymphoma; IPI, International Prognostic Index; LC3, Protein light chain 3; mTOR, mammalian target of rapamycin; FFPE, Paraffin-embedded; RAPA, rapamycin; VDR, vitamin D receptor

Key words: 1,25(OH)₂D₃, autophagy, DLBCL, mTOR, CYP24A1

p27 (5-7). AKT can indirectly activate mammalian target of rapamycin (mTOR), a serine/threonine kinase downstream of the PI3K/AKT pathway (8). Activated mTOR can increase the phosphorylation levels of the translational repressor eukaryotic translation initiation factor 4E-binding protein 1 (4EBP1) and ribosomal protein S6 kinase β -1 (p70S6K), which increases mRNA translation, protein synthesis and cell proliferation (9,10). Therefore, mTOR is able to influence cell cycle progression and the homeostasis of metabolism, and enhance cell growth. The PI3K/AKT-mTOR axis also plays an important role in the negative regulation of autophagy (11). Previous studies have reported the aberrant activation of the PI3K/AKT/mTOR pathway, and its role in controlling tumor cell proliferation and survival in DLBCL (4,8). Moreover, patients with DLBCL with active PI3K/AKT/mTOR signaling experience a more rapid deterioration, with poor treatment response and shortened survival times (12). The suppression of active PI3K/AKT/mTOR signaling has been studied, and several inhibitors have been discovered; mTOR inhibitors have been shown to be effective in preclinical and clinical settings for the treatment of autoimmune diseases, cancer and infectious diseases, such as HIV (13-24). Furthermore, dual inhibitors of PI3K and mTOR, including GSK2126458A and NVP-BEZ235, are being developed for cancer that show promising chemotherapeutic profiles in different settings (25-27). However, the mTOR inhibitor rapamycin (RAPA) and other analogues, such as everolimus, exhibit various side effects, including stomatitis, rashes, myelosuppression and metabolic complications, such as hyperglycemia, hypertriglyceridemia, hypercholesterolemia and fatigue (28,29). In the case of serious side effects, dose adjustment, interruption or permanent discontinuation are required to reduce the toxicity of these medications (28). The combination of RAPA or other analogues with additional medications to reduce toxicity may be an effective way to treat cancer.

1,25-Dihydroxyvitamin D₃ [1,25(OH)₂D₃] has an important role in bone homeostasis and calcium metabolism (30,31). Furthermore, 1,25(OH)₂D₃ has been shown to have antiproliferative and proapoptotic effects, and promote differentiation in cancer cells, including pancreatic, breast and prostate cancer (32-38). 1,25(OH)₂D₃ inhibits the mTOR signaling pathway by stimulating the expression of DNA damage-inducible transcript 4 (DDIT4), a potent suppressor of mTOR activity (39). This may be a novel strategy for the treatment of cancer. 1,25(OH)₂D₃ induces autophagy in SH-SY5Y cells to attenuate rotenone-induced neurotoxicity (40) and inhibits the proliferation of keratinocytes by suppressing the mTOR signaling pathway (41). However, whether 1,25(OH)₂D₃ inhibits the progression of DLBCL by suppressing the mTOR signaling pathway is unclear.

The concentration of 1,25(OH)₂D₃ available in tissues depends on the balance between its synthesis and degradation, carried out by 25-hydroxyvitamin D-1 α hydroxylase and 25-hydroxyvitamin D-24-hydroxylase (CYP24A1), respectively. A previous study found that the basal expression of CYP24A1 was higher in several tumor types, including colon, breast, lung, ovarian and cervical tumors (42). The high expression of CYP24A1 was found to be associated with the increased expression of replication licensing factors and tumor progression (43-47). However, little is known concerning the

relationship between the clinical features of patients with DLBCL and the expression of CYP24A1, or how the anti-tumor effect of 1,25(OH)₂D₃ in DLBCL is influenced by the expression of CYP24A1.

The present study aimed to investigate the relationship between the clinical features of patients with DLBCL and the expression of CYP24A1. In addition, the roles of the PI3K/AKT/mTOR signaling pathway and autophagy in the anticancer effects of 1,25(OH)₂D₃ in DLBCL cells were investigated.

Materials and methods

Reagents. 1,25(OH)₂D₃ and RAPA were purchased from Sigma-Aldrich; Merck KGaA. 3-Methyladenine was purchased from Selleck Chemicals. The FITC Annexin V Apoptosis Detection kit, propidium iodide (PI) and ribonuclease A (RNase A) were purchased from BD Biosciences. The Cell Counting Kit-8 (CCK-8) was purchased from 7Sea Biotech. The ECL Western kit was purchased from Advanta, Inc. The following primary antibodies were purchased from Cell Signaling Technology, Inc.: mTOR (cat. no. 2972), phosphorylated (p)-mTOR (Ser2448; cat. no. 2971), AKT (cat. no. 4691), p-AKT (Ser473; cat. no. 4060), p-4EBP1 (Thr37/46; cat. no. 2855), 4E-BP1 (cat. no. 9452), p-p70S6K (Thr389; cat. no. 9234), p70S6K (cat. no. 2708), ubiquitin binding protein P62 (P62; cat. no. 8025), LC3I/II (cat. no. 4108). The goat monoclonal antibody against CYP24A1 was purchased from Abcam (cat. no. ab189322). A rabbit monoclonal antibody against the vitamin D receptor (VDR) was purchased from Santa Cruz Biotechnology (cat. no. sc-13133), Inc. α -Tubulin was purchased from ProteinTech Group (cat. no. 11224-1-AP), Inc. Horseradish peroxidase (HRP)-conjugated goat-anti-mouse IgG (cat. no. A-11001) and HRP-conjugated goat-anti-rabbit IgG (cat. no. A-11034) were obtained from Thermo Fisher Scientific, Inc. 1,25(OH)₂D₃ was dissolved and stored in ethanol and RAPA was dissolved and stored in DMSO at -20°C. A biotinylated goat-anti-mouse antibody (cat. no. PV-9003) was purchased from Origene Technologies, Inc. A fluorescein-conjugated goat anti-rabbit secondary antibody (cat. no. Andy Fluor™ 594) was purchased from GeneCopoeia, Inc. Fetal calf serum was purchased from Biological Industries.

Clinical specimens. In total, 57 formalin-fixed (overnight at 4°C), paraffin-embedded (FFPE) DLBCL lymph node tissues from diagnostic biopsies (age, 31-70 years; male:female, 30:27) and 21 FFPE lymph node tissues from diagnostic biopsies (age, 35-66 years; male:female, 12:9) were collected. All the samples were obtained between January 2010 to June 2013 from Xiangya Hospital. The Institutional Ethical Review Board of Xiangya Hospital approved the present study and written informed consent was obtained from all patients for the use of their biopsy samples. No patient had received any antitumor treatments before the biopsy sample was collected. The Ann Arbor staging system was used to assess the stage of the patient and the International Prognostic Index (IPI) was used to assess the risk of the patient (48). The serum lactate dehydrogenase (LDH) level was measured by clinical laboratory staff using the Hitachi 7170 biochemical analyzer (Hitachi, Ltd.).

Cell culture. The human Pfeiffer DLBCL cell line was purchased from the American Type Culture Collection (cat. no. ATCC® CRL-2632™) and cultured in RPMI-1640 (HyClone; GE Healthcare Life Sciences) supplemented with 10% FBS (Gibco; Thermo Fisher Scientific, Inc.) and 100 U/ml penicillin and streptomycin (HyClone; GE Healthcare Life Sciences) at 37°C in a humidified 5% CO₂ incubator. Cells were passaged every 2-3 days to maintain a density between 1-2x10⁶ cells/ml.

Immunohistochemistry. Sections (thickness, 4 μm) obtained from the 57 FFPE DLBCL specimens were deparaffinized, rehydrated and the endogenous peroxidase activity was blocked using 3% H₂O₂ in methanol for 15 min at room temperature. The sections were microwaved for 4 min with trisodium citrate dihydrate solution (0.125%, pH 6.0) and then soaked with PBS three times for 5 min for citrate-mediated high-temperature antigen retrieval. Non-specific binding was blocked by pre-incubating with 5% BSA for 30 min at room temperature. Sections were incubated with anti-CYP24A1 (1:300) at 4°C overnight and then incubated with a biotinylated secondary antibody (1:5,000) for 30 min at room temperature. Sections were incubated with a streptavidin-HRP complex (Origene Technologies, Inc.) at room temperature for 5 min and 3,3'-diaminobenzidine (Origene Technologies, Inc.) at room temperature for 5 min, sections were then counterstained with hematoxylin at room temperature for 20. Positive cells were counted in 10 randomly selected fields with a x40 objective (Olympus CX23; Olympus Corporation). All sections were scored by two pathologists. The staining index was calculated as the product of staining intensity (Score: 0, no staining; 1, weak/light yellow; 2, moderate/yellow-brown; 3, strong/brown). The number of stained cells was scored as 0 (0-5%), 1 (6-25%), 2 (26-50%), 3 (51-75%) or 4 (76-100%). The sum of the intensity and number scores was used as the final staining score (0-7). Low expression was defined as a final staining score of ≤3. High expression was defined as a final staining score >3.

Cell viability assay. Pfeiffer cells in exponential phase growth were plated at a density of 1x10⁴ cells/well in 96-well plates. The wells were divided into three groups (five wells/group): Control group (0.1% ethanol); 10 nM 1,25(OH)₂D₃ group; 100 nM 1,25(OH)₂D₃ group. The concentrations of 1,25(OH)₂D₃ used were similar to previous studies (49,50). Cytotoxicity was determined using the CCK-8 assay, according to the manufacturer's instructions. After 48 h of treatment, cells were incubated with 10 μl CCK-8 reagent for a further 3 h. The optical density of the samples was determined using a microplate reader at 450 nm. Each experiment was performed in triplicate.

Cell cycle analysis. Pfeiffer cells were plated into 6-well plates at a density of 3x10⁵ cells/well and divided into six groups: Control group (0.1% ethanol); 10 nM 1,25(OH)₂D₃; 100 nM 1,25(OH)₂D₃; 10 nM RAPA; combination group (10 nM or 100 nM 1,25(OH)₂D₃ + 10 nM RAPA). After incubation for 48 h, the cells were washed twice with PBS and fixed with ice-cold 70% ethanol at -20°C overnight. Subsequently, the cells were centrifuged at 111.8 x g for 5 min at 4°C, washed once

with PBS and the DNA was labeled with 0.5 ml cold PI solution (0.1% Triton X-100, 0.1 mM EDTA, 50 μg/ml RNase A, 50 μg/ml PI in PBS) on ice for 30 min in the dark. The cell cycle distribution was determined using a FACSCalibur flow cytometer (BD Biosciences) using ModFit LT software version 3.0 (Verity Software House).

LC3II immunofluorescence staining. Cells were fixed for 15 min with 4% paraformaldehyde at 4°C and permeabilization with 0.25% Triton X-100 in PBS for 5 min at room temperature. After blocking with fetal calf serum for 1 h at room temperature, the slides were incubated with an LC3/II primary antibody (1:200) overnight at 4°C. The slides were then incubated with a fluorescein-conjugated goat anti-rabbit secondary antibodies (1:1,000) for 1 h at 37°C. The nuclei of cells were stained using DAPI (1 μg/ml) at room temperature. The fluorescent staining was imaged using a confocal microscope (IX71; Olympus Corporation). In total, 10 random fields were selected for analyzed (magnification, x400 and x600).

Transmission electron microscopy. To morphologically observe the induction of autophagy in 1,25(OH)₂D₃ treated Pfeiffer cells, ultrastructural analysis was performed. After treatment with 100 nM 1,25(OH)₂D₃ for 48 h, cells were washed twice with PBS and fixed with ice-cold glutaraldehyde (3% in 0.1 M cacodylate buffer, pH 7.4) for 30 min. Cells were post-fixed in 1% osmium tetroxide at room temperature for 2 h and embedded in Epon812 (SERVA Electrophoresis GmbH) before being cut (60 nm) and stained with 2% uranyl acetate/2.5% lead citrate and incubated for 15 min at room temperature. The formation of autophagosomes was assessed using the Tecnai electron microscope (FEI; Thermo Fisher Scientific, Inc.) at a magnification of x1,700 and x5,000.

Western blot analysis. Proteins were extracted using a nuclear and cytoplasmic protein extraction kit (Beyotime Institute of Biotechnology). Protein concentrations were determined using the bicinchoninic acid method. Proteins (30 μg) were separated using 6% SDS-PAGE under reducing conditions and then transferred onto PVDF membranes. The membranes were blocked in 5 mg/ml BSA for 2 h at room temperature. The following primary antibodies were used: VDR (1:1,000), CYP24A1 (1:1,000), AKT (1:1,000), p-AKT (1:1,000), mTOR (1:1,000), p-mTOR (1:1,000), LC3II (1:1,000) and P62 (1:1,000), P70S6K (1:1,000), p-p70S6K (1:1,000), 4EBP1 (1:1,000) and p-4EBP1 (1:1,000). α-Tubulin (1:5,000) was used as a loading control. The primary antibodies were incubated with the membranes overnight at 4°C. HRP-conjugated secondary antibodies (1:5,000) were incubated with the membranes at room temperature for 1-2 h. Protein bands were visualized using ECL and the Chemi Doc™ MP Imaging System (Bio-Rad Laboratories, Inc.). Band densitometry was assessed using ImageJ software 1.8.0 (National Institutes of Health).

Statistical analysis. All statistical analysis was performed using SPSS 22.0 software (IBM Corp.). Data are present as the mean ± SD. Data were analyzed using the χ² test, Student's t-test, or one- or two-way ANOVA and the Tukey's test when applicable. Data were representative of three independent

experiments. $P < 0.05$ was considered to indicate a statistically significant difference.

Results

Expression of CYP24A1 is different in patients with DLBCL and lymphnoditis. To examine whether the expression of CYP24A1 protein in DLBCL and lymphnoditis tissues, immunohistochemistry was performed on the 57 paraffin-embedded DLBCL lymph node tissue sections and 21 lymphnoditis lymph node tissue sections to evaluate the expression of CYP24A1 (Fig. 1A-D). High levels of CYP24A1 expression were detected in 9.5% of patients with lymphnoditis ($n=21$), whereas high levels of CYP24A1 expression were detected in 35.1% of patients with DLBCL ($n=57$). Low CYP24A1 expression was detected in 90.5% of patients with lymphnoditis, while low CYP24A1 expression was detected in 74.9% of patients with DLBCL. The expression levels of CYP24A1 between patients with lymphnoditis and DLBCL was significantly different ($P < 0.001$). The patients with DLBCL were stratified into different groups, using factors such as age and sex, to investigate associations with the expression of CYP24A1 (Table I). There was no significant different in the expression of CYP24A1 between the Ann Arbor stage I/II patients and the Ann Arbor stage III/IV patients ($P=0.28$), however, the expression of CYP24A1 was significantly higher in patients with a higher IPI ($P < 0.05$). Serum LDH levels were also significantly associated with CYP24A1 expression. The patient whose clinical treatment response was stable or showed complete remission had a lower level of CYP24A1 ($P < 0.05$). The expression of CYP24A1 was significantly higher in patients over the age of 60 ($P < 0.05$).

1,25(OH)₂D₃ inhibits the proliferation of Pfeiffer cells. To investigate the growth inhibitory properties of 1,25(OH)₂D₃, CCK-8 assays were performed, which is based on the ability of viable cells to reduce CCK-8 to formazan crystals. As shown in Fig. 1E, Pfeiffer cell proliferation was significantly inhibited by 10 nM ($P < 0.01$) and 100 nM 1,25(OH)₂D₃ ($P < 0.001$). The rate of inhibition was calculated as $16.8 \pm 3.4\%$ for cells treated with 10 nM 1,25(OH)₂D₃ and $28.2 \pm 2.9\%$ for cells treated with 100 nM 1,25(OH)₂D₃ for 48 h.

1,25(OH)₂D₃ induces cell cycle arrest in Pfeiffer cells. To determine whether 1,25(OH)₂D₃ induces cell cycle arrest in Pfeiffer cells, the effect of 1,25(OH)₂D₃ on the cell cycle distribution was analyzed using PI staining. Pfeiffer cells were treated with different concentrations of 1,25(OH)₂D₃ for 48 h and then subjected to cell cycle analysis. As shown in Fig. 2A and B, $22.70 \pm 0.40\%$ of cells in the control group were in the G1 phase, while the cells treated with 100 nM 1,25(OH)₂D₃ showed a significant increase in the proportion of cells in the G1 phase ($26.11 \pm 0.64\%$; $P < 0.05$). In addition, whether 1,25(OH)₂D₃ increased the G1 phase arrest induced by RAPA was investigated. It was found the addition of RAPA increased the number of cells in the G1 phase compared with 1,25(OH)₂D₃ treatment alone (Table II; Fig. 2A and B).

1,25(OH)₂D₃ induced the expression of CYP24A1 mediated by VDR, which is the receptor of 1,25(OH)₂D₃, and

Table I. Clinical features and CYP24A1 expression of patients with diffuse large B cell lymphoma.

Parameter	CYP24A1 expression		P-value
	Low	High	
Age, years			
<60	32	11	0.008 ^a
≥60	5	9	
Sex			
Male	18	12	0.37
Female	19	8	
Ann Arbor stage			
I/II	10	3	0.28
III/IV	27	17	
LDH			
Normal	32	11	0.015 ^a
Elevated	5	9	
IPI			
0-2	18	8	0.008 ^a
3-5	19	20	
Clinical treatment response			
CR/PR	26	8	0.028 ^a
SD/PD	11	12	

The χ^2 test was used to compare the distribution of clinical features between low- and high-level CYP24A1 expression. ^a $P < 0.05$. CYP24A1, 25-hydroxyvitamin D-24-hydroxylase; LDH, serum lactate dehydrogenase; IPI, International Prognostic Index; CR, complete remission; PR, partial remission; SD, stable disease; PD, progressive disease.

Table II. Cell cycle distribution of Pfeiffer cells treated with 1,25(OH)₂D₃ and RAPA.

Group	G1 phase (%)
Control	22.70 ± 0.40
10 nM 1,25(OH) ₂ D ₃	22.92 ± 0.93
100 nM 1,25(OH) ₂ D ₃	26.11 ± 0.64^a
10 nM RAPA	$35.74 \pm 0.55^{a,b}$
10 nM RAPA + 10 nM 1,25(OH) ₂ D ₃	$37.13 \pm 0.75^{a,b}$
10 nM RAPA + 100 nM 1,25(OH) ₂ D ₃	$42.75 \pm 0.61^{a,c}$

The differences between G1 phase populations were analyzed using the Tukey's post hoc test. ^a $P < 0.05$ vs. control; ^b $P < 0.05$ vs. 100 nM 1,25(OH)₂D₃; ^c $P < 0.05$ vs. 10 nM RAPA. RAPA, rapamycin; 1,25(OH)₂D₃, 1,25-dihydroxyvitamin D₃.

CYP24A1 causes the degradation of 1,25(OH)₂D₃. This is an important regulatory mechanism to control the level of 1,25(OH)₂D₃ (30,31). In order to investigate whether RAPA increases the cell cycle arrest induced by 1,25(OH)₂D₃,

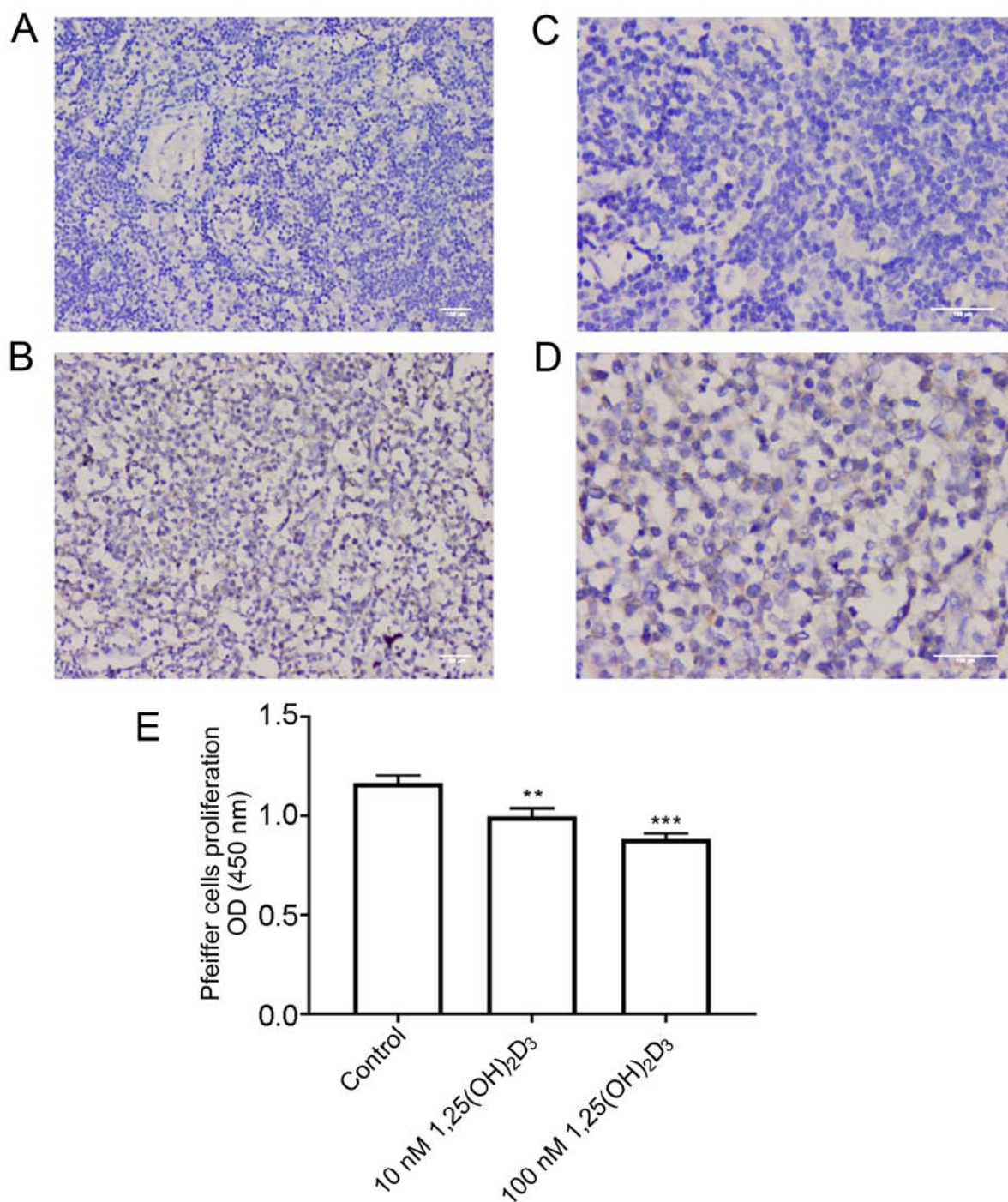


Figure 1. CYP24A1 is differently expressed in patients with DLBCL and lymphnoditis, and 1,25(OH)₂D₃ inhibits the proliferation of Pfeiffer cells. Sections of paraffin-embedded lymph node tissues from the diagnostic biopsies of 20 patients with lymphnoditis and 57 patients with DLBCL were processed for immunohistochemical staining with an antibody against CYP24A1. Representative images of CYP24A1 immunohistochemical staining in lymphnoditis samples at (A) x200 and (C) x400 magnification. Representative images of CYP24A1 immunohistochemical staining in DLBCL lymph node tissue at (B) x200 and (D) x400 magnification. Scale bar, 100 μm. (E) Pfeiffer cells were cultured with 1,25(OH)₂D₃ (10-100 nM) for 48 h. After treatment, cell viability was determined using a Cell Counting Kit-8. Pfeiffer cell proliferation was significantly inhibited by 10 and 100 nM 1,25(OH)₂D₃. The rate of inhibition was calculated to be 16.8±3.4% for cells treated with 10 nM 1,25(OH)₂D₃ and 28.2±2.9% for cells treated with 100 nM 1,25(OH)₂D₃ for 48 h. Each experiment was performed in triplicate. **P<0.01, ***P<0.001 vs. control. CYP24A1, 25-hydroxyvitamin D-24-hydroxylase; 1,25(OH)₂D₃, 1,25-dihydroxyvitamin D₃; OD, optical density; DLBCL, diffuse large B cell lymphoma.

by reducing the degradation of 1,25(OH)₂D₃, the levels of CYP24A1 and VDR were determined in Pfeiffer cells after exposure to either 1,25(OH)₂D₃ or RAPA using western blot analysis. It was found that RAPA suppressed the expression of CYP24A1 and VDR induced by 1,25(OH)₂D₃ (Fig. 2C and D). This suggested that RAPA increased the cell cycle arrest in

Pfeiffer cells induced by 1,25(OH)₂D₃ by suppressing the expression of CYP24A1 and VDR.

1,25(OH)₂D₃ induces autophagy in Pfeiffer cells. In order to investigate whether 1,25(OH)₂D₃ regulates autophagy in Pfeiffer cells, the induction of autophagy was analyzed. The

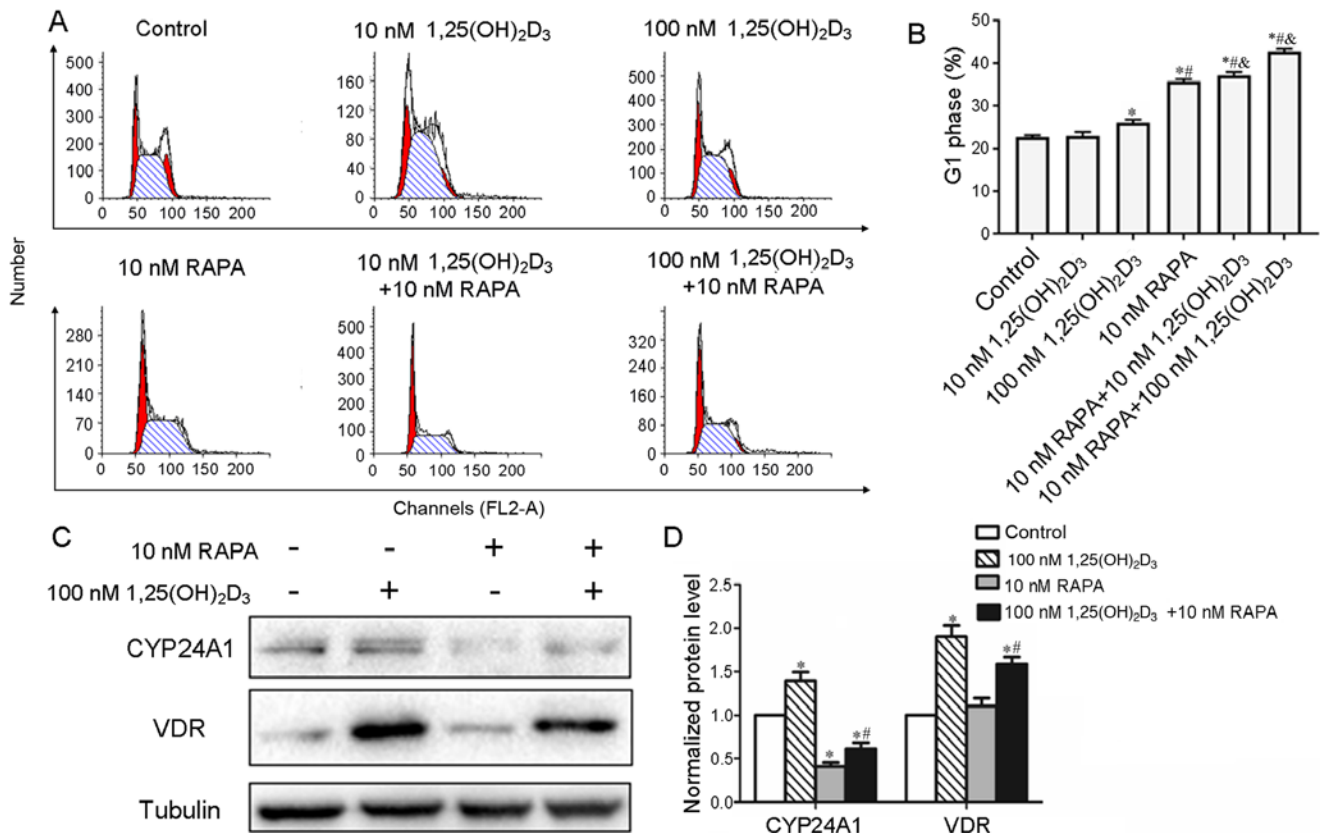


Figure 2. Cell cycle distribution of Pfeiffer cells after treatment with 1,25(OH)₂D₃ and RAPA, and the expression of CYP24A1 and VDR in Pfeiffer cells. (A) Pfeiffer cells were cultured with 10 or 100 nM 1,25(OH)₂D₃ and RAPA (10 nM). After 48 h, the cell cycle distribution was analyzed. The figure shows representative examples of three independent experiments. (B) Quantification of the G1 population of Pfeiffer cells. (C) After treatment with 1,25(OH)₂D₃ and/or RAPA for 48 h, cells were harvested and the protein levels of CYP24A1 and VDR were analyzed via western blotting. A representative of three independent experiments is shown. (D) Quantification of western blotting results. *P<0.05 vs. control; #P<0.05 vs. 100 nM 1,25(OH)₂D₃; &P<0.05 vs. 10 nM RAPA. VDR, vitamin D receptor; CYP24A1, 25-hydroxyvitamin D-24-hydroxylase; 1,25(OH)₂D₃, 1,25-dihydroxyvitamin D₃; RAPA, rapamycin.

induction of autophagy in Pfeiffer cells after treatment with or without 1,25(OH)₂D₃ (10 nM, 100 nM) for 48 h was analyzed. The extent of autophagosome formation is associated with the modification of LC3I to LC3II and the degradation of P62. A significant increase in LC3II/LC3I and a reduction in P62 was induced by 100 nM 1,25(OH)₂D₃, as assessed using western blot analysis (Fig. 3C and D). Furthermore, the aggregation and localization of LC3 plays an important role in the maturation and transport of the autophagosome; therefore, immunofluorescence experiments were performed to observe changes in LC3 aggregation. A notable increase in green LC3 puncta was observed in the 100 nM 1,25(OH)₂D₃ treatment group compared with the control group (Fig. 3B). In addition, it was found that 100 nM 1,25(OH)₂D₃ enhanced the formation of autophagosomes, as observed using transmission electron microscopy (Fig. 3A). These findings indicated that 1,25(OH)₂D₃ activates autophagy in Pfeiffer cells.

1,25(OH)₂D₃ inhibits the AKT/mTOR signaling pathway. Having established that 1,25(OH)₂D₃ inhibited proliferation and induced autophagy in Pfeiffer cells, the molecular mechanisms underlying these biological effects were investigated. Activation of the AKT/mTOR signaling pathway increases the proliferation of Pfeiffer cells and is one of the major targets in the process of autophagy (51). Western blot analysis showed that p-AKT and p-mTOR were downregulated after

1,25(OH)₂D₃ exposure. The activation of downstream targets of mTOR, including p70S6K and 4EBP1, were also decreased following 1,25(OH)₂D₃ treatment (Fig. 3E and F).

Discussion

In the present study, it was found that the levels of CYP24A1 in DLBCL lymph node tissues were higher than in lymph node tissues. There was no significant difference in the expression of CYP24A1 between Ann Arbor stage I/II patients and Ann Arbor stage III/IV patients (P=0.28), however, the expression of CYP24A1 was significantly higher in patients with a higher IPI. Moreover, CYP24A1 expression was negatively associated with clinical treatment response. Patients over the age of 60 had a higher level of CYP24A1 expression. Furthermore, it was found 1,25(OH)₂D₃ inhibited proliferation and increased the G1 phase population of Pfeiffer cells. RAPA led to a further increase in the G1 population and decreased the expression of CYP24A1 and VDR induced by 1,25(OH)₂D₃. 1,25(OH)₂D₃ induced the formation of autophagosomes and increased the levels of the autophagy related protein LC3II/LC3I and reduced the expression of P62. In addition, 1,25(OH)₂D₃ decreased the phosphorylation of AKT, mTOR, and its downstream targets 4EBP and p70S6K in Pfeiffer cells.

To the best of our knowledge, the present study was the first to show higher levels of the vitamin D-degrading enzyme

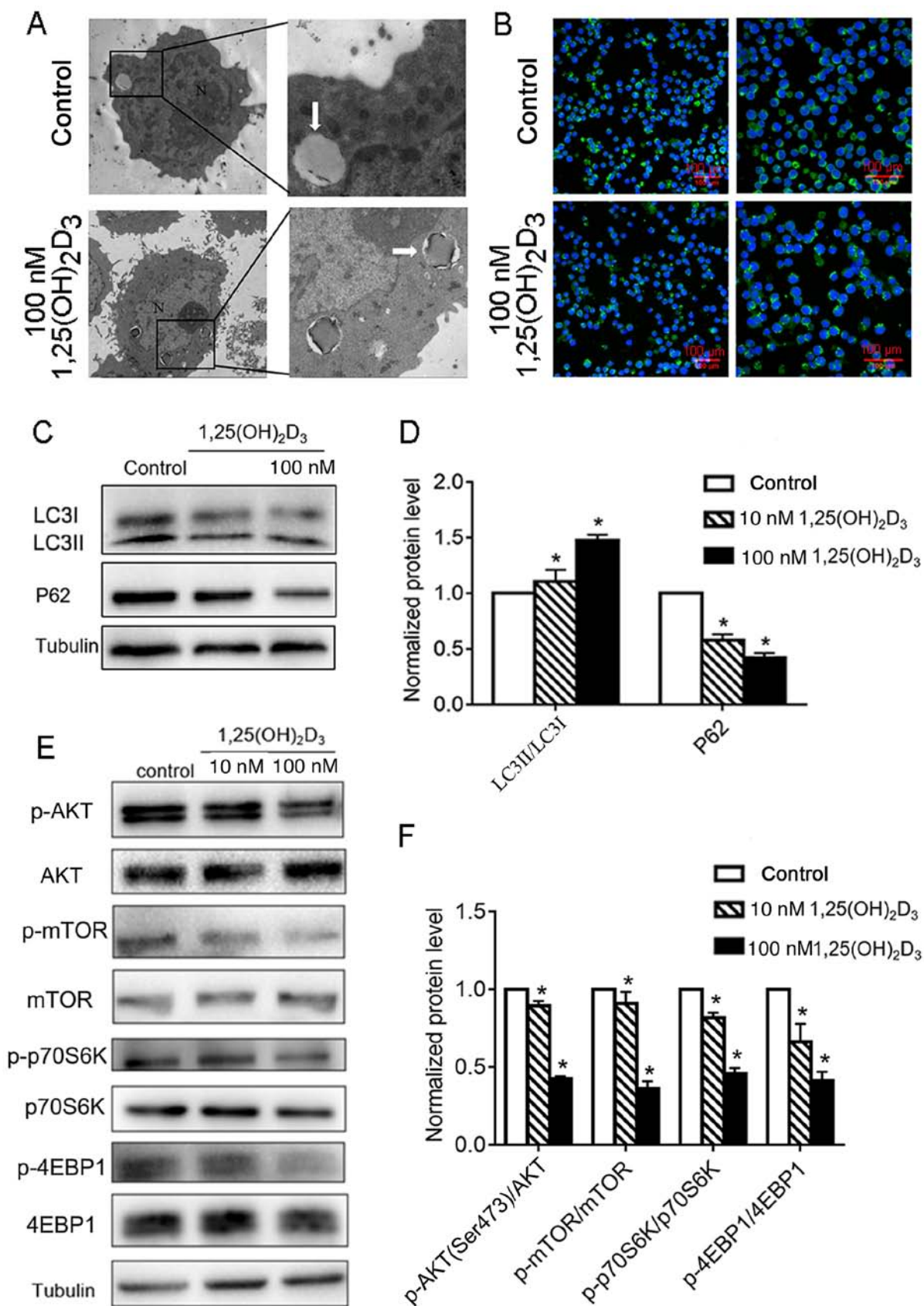


Figure 3. Analysis of autophagy and the AKT/mTOR signaling pathway in Pfeiffer cells after treatment with 1,25(OH)₂D₃. (A) Representative transmission electron microscope images [magnification, x1,700 (left) and x5,000 (right)] of the ultrastructure of Pfeiffer cells after treatment with or without 100 nM 1,25(OH)₂D₃ for 48 h. (B) Changes in the level and localization of LC3 examined by confocal microscopy after treatment with or without 100 nM 1,25(OH)₂D₃ for 48 h. Scale bar = 100 μm. (C) Western blot analysis of the expression of the autophagy related proteins LC3 and P62 after treatment with 100 nM 1,25-D₃ for 48 h and (D) the quantification. (E) Pfeiffer cells were cultured without or with 1,25(OH)₂D₃ for 1 h. The phosphorylation levels of AKT/mTOR signaling proteins were evaluated using western blotting. A representative example of three independent experiments is shown. (F) Quantification of western blotting. *P < 0.05 vs. control. LC3, protein light chain 3; 1,25(OH)₂D₃, 1,25-dihydroxyvitamin D₃; mTOR, target of rapamycin; p-, phosphorylated; 4EBP, eukaryotic translation initiation factor 4E-binding protein 1; p70S6K, ribosomal protein S6 kinase β-1; P62, ubiquitin binding protein P62.

CYP24A1 in DLBCL tissues compared with lymph node tissues, which was used as a normal control for the lymphoma tissues. CYP24A1 degrades 1,25(OH)₂D and 25(OH)D, which is a substrate required for the synthesis of 1,25(OH)₂D. Therefore, CYP24A1 is an important factor in determining the local concentration of 1,25(OH)₂D and regulates the antiproliferative effect of 1,25(OH)₂D (52). The higher expression of CYP24A1 may be one explanation for the significantly lower serum concentration of 25(OH)D in patients with DLBCL (53). In addition, previous studies have described the moderate impact of 1,25(OH)₂D on the proliferation of certain DLBCL cell lines, including DOHH2 and K442 (50,49). The present study found higher levels of CYP24A1 expression in DLBCL lymph node tissues, suggesting that the actual concentration of vitamin D available and the concentration of 1,25(OH)₂D in these tissues may be low, and that this may attenuate the antitumor effects of 1,25(OH)₂D *in vivo*. The increased expression of CYP24A1 was also found in some solid tumors, including colon, lung, prostate, thyroid, breast and ovarian cancer cells (43-47). However, little is known regarding the mechanism underlying the increased expression of CYP24A1 in these cancer cells. Understanding the mechanism that leads to the upregulation of CYP24A1 in tumors may provide strategies for targeting CYP24A1 in the future. A combination of CYP24A1 inhibitors, such as liarozole, genistein [a soy isoflavone that directly inhibits CYP24A1 activity and increases the sensitivity of cells to 1,25(OH)₂D] or ritonavir (which inhibits the expression of CYP24A1), may increase the level and calcemic activity of 1,25(OH)₂D, increasing the risk of hypercalcemic side effects (54,55). Structural non-calcemic action analogs of calcitriol that resist CYP24A1 may be more biologically active and more useful in cancer therapy and for the treatment of DLBCL, which expresses a high level of CYP24A1.

In the present study, it was found that 1,25(OH)₂D₃ inhibits the proliferation of DLBCL Pfeiffer cell line. In a previous study into the antiproliferative effect of 1,25(OH)₂D₃ in other DLBCL cell lines, 1,25(OH)₂D₃ was found to have an antiproliferative effect on the Pfeiffer cell line (50).

CYP24A1, which degrades 1,25(OH)₂D₃ and 25(OH)D, is important for lowering the levels of 1,25(OH)₂D₃ and 25(OH)D. Vitamin D deficiency is a risk factor for autoimmune diseases, such as rheumatoid arthritis and system lupus erythematosus (SLE) (56,57). A recent study reported that vitamin D deficiency and the upregulation of CYP24A1 have a combined role in the transition to SLE (58). Patients with autoimmune diseases, in particular those mediated by B lymphocytes, have a higher risk of developing DLBCL, with a more aggressive nature, possibly due to the misregulated production of several cytokines, including interleukin (IL)-6, IL-10 and tumor necrosis factor- α , that contribute to the pathogenesis of DLBCL (59-62). 1,25(OH)₂D₃ also plays an important role in the regulation of immune function by inhibiting the production of cytokines (63,64). In future research, whether the increased production of cytokines contribute to the pathogenesis of DLBCL, and whether this is associated with the upregulation of CYP24A1, should be investigated. Furthermore, whether inhibiting the production of cytokines using 1,25(OH)₂D₃ is beneficial for the treatment of some cases of DLBCL should be investigated in *in vivo* studies.

Autophagic cell death is a survival mechanism to deal with metabolic stress and is a caspase-independent mechanism of cell death (65). Nevertheless, previous studies have indicated that autophagy and apoptosis may be interconnected process (66,67). The present study found that 1,25(OH)₂D₃ induced autophagy in Pfeiffer cells. These results suggested that 1,25(OH)₂D₃ induced cell killing in a caspase-independent autophagy-mediated manner in Pfeiffer cells.

Activation of the PI3K/AKT/mTOR signaling pathway suppresses autophagy (68,69). The data from the present study showed that 1,25(OH)₂D₃ decreased the phosphorylation levels of AKT and mTOR in Pfeiffer cells, consistent with a previous study that found that 1,25(OH)₂D₃ is involved in mTOR signaling (70). These results suggested that 1,25(OH)₂D₃ induces autophagy in Pfeiffer cells by inhibiting the PI3K/AKT/mTOR signaling pathway. In addition, the PI3K/AKT/mTOR signaling pathway also increases mRNA translation, protein synthesis and cellular proliferation (9,10). The aberrant activation of mTOR is frequently associated with poorer prognosis and has been well described in non-Hodgkin lymphoma (4,71-73). Suppressing mTOR in Pfeiffer cells may extend the therapeutic applications of 1,25(OH)₂D to the treatment of DLBCL. A previous study reported that 1,25(OH)₂D₃ inhibits the mTOR signaling pathway by stimulating the expression of DDIT4, a potent suppressor of mTOR activity (39). The present study showed that 1,25(OH)₂D₃ decreased the phosphorylation of downstream factors in the PI3K/AKT/mTOR signaling pathway in Pfeiffer cells, including 4EBP and p70S6K. p70S6K is an important regulator of protein synthesis; blocking the activation of p70S6K, for example using Saquinavir-NO, interrupts protein synthesis, leading to decreased cancer cell proliferation (74-77). The inhibition of Pfeiffer cell proliferation by 1,25(OH)₂D₃ may be due to the decreased phosphorylation of p70S6K. In future studies, the anticancer effects of other p70S6K inhibitors should be investigated in DLBCL, and their potential synergism with 1,25(OH)₂D₃ should be tested.

A previous study reported that the mTOR signaling inhibitor RAPA and its analogs increase the antitumor effects of 1,25(OH)₂D in breast cancer cells and acute myelogenous leukemia (78,79). This effect of RAPA and its analogs may be due to the increased expression, or nuclear translocation, of VDR (79). Consistent with these previous studies, the data from the present study showed that 1,25(OH)₂D₃ increased the G1 phase population of Pfeiffer cells and that this was potentiated by RAPA. However, it was found that RAPA blocked the increase in VDR and CYP24A1 expression induced by 1,25(OH)₂D₃. 1,25(OH)₂D₃ induced the expression of CYP24A1, mediated by VDR, which is the receptor of 1,25(OH)₂D₃, and CYP24A1 causes the degradation of 1,25(OH)₂D₃. This is an important autoregulatory mechanism of 1,25(OH)₂D₃. RAPA may potentiate the effect of 1,25(OH)₂D₃ by reducing its degradation.

In conclusion, the results of the present study suggested that the expression of CYP24A1 may be a novel prognostic indicator for DLBCL. 1,25(OH)₂D₃ inhibited the proliferation, and induced the autophagy, of Pfeiffer cells. In addition, 1,25(OH)₂D₃ increased the G1 phase population of Pfeiffer cells. These effects may be mediated by inhibiting the PI3K/AKT/mTOR signaling pathway. RAPA may potentiate

the cell cycle arrest caused by 1,25(OH)₂D₃ by inhibiting the expression of CYP24A1 and VDR.

Acknowledgements

Not applicable.

Funding

The present study was supported by the National Natural Science Foundation of China (grant no. 81570200) and was partially supported by the fund from Guangzhou Institute of Pediatrics/Guangzhou Women and Children's Medical Center (grant no. YIP-2018-005). The funders had no role in the study concept, study design, data analysis, interpretation or reporting of the results. The authors had full control of the data and information submitted for publication.

Availability of data and materials

The datasets used and/or analyzed during the current study are available from the corresponding author on reasonable request.

Authors' contributions

WW and JH contributed to the design of the study and were involved in performing the experiments, data analysis and the preparation of the manuscript. YT contributed to the data analysis. MZ contributed to data analysis and manuscript preparation. All authors contributed to the data interpretation and approved the final version of the manuscript. All authors read and approved the manuscript.

Ethics approval and consent to participate

The Institutional Ethical Review Board of the Xiangya Hospital approved the present study, and written informed consent was obtained from all patients for the use of their biopsy samples.

Patient consent for publication

Not applicable.

Competing interests

The authors declare that they have no competing interests.

References

- Li S, Young KH and Medeiros LJ: Diffuse large B-cell lymphoma. *Pathology* 50: 74-87, 2018.
- Li JM, Wang L, Shen Y, Xia ZG, Chen Y, Chen QS, Chen Y, Zeng XY, You JH, Qian Y and Shen ZX: Rituximab in combination with CHOP chemotherapy for the treatment of diffuse large B cell lymphoma in Chinese patients. *Ann Hematol* 86: 639-645, 2007.
- He F, Wang L, Hu XB, Yin DD, Zhang P, Li GH, Wang YC, Huang SY, Liang YM and Han H: Notch and BCR signaling synergistically promote the proliferation of Raji B-lymphoma cells. *Leuk Res* 33: 798-802, 2009.
- Uddin S, Hussain AR, Siraj AK, Manogaran PS, Al-Jomah NA, Moorji A, Atizado V, Al-Dayel F, Belgaumi A, El-Solh H, *et al*: Role of phosphatidylinositol 3'-kinase/AKT pathway in diffuse large B-cell lymphoma survival. *Blood* 108: 4178-4186, 2006.
- Liang J, Zubovitz J, Petrocelli T, Kotchetkov R, Connor MK, Han K, Lee JH, Ciarallo S, Catzavelos C, Beniston R, *et al*: PKB/Akt phosphorylates p27, impairs nuclear import of p27 and opposes p27-mediated G1 arrest. *Nat Med* 8: 1153-1160, 2002.
- Héron-Milhavet L, Franckhauser C, Rana V, Berthenet C, Fisher D, Hemmings BA, Fernandez A and Lamb NJ: Only Akt1 is required for proliferation, while Akt2 promotes cell cycle exit through p21 binding. *Mol Cell Biol* 26: 8267-8280, 2006.
- Brazil DP, Yang ZZ and Hemmings BA: Advances in protein kinase B signalling: AKTion on multiple fronts. *Trends Biochem Sci* 29: 233-242, 2004.
- Cai SL, Tee AR, Short JD, Bergeron JM, Kim J, Shen J, Guo R, Johnson CL, Kiguchi K and Walker CL: Activity of TSC2 is inhibited by AKT-mediated phosphorylation and membrane partitioning. *J Cell Biol* 173: 279-289, 2006.
- Cantley LC: The phosphoinositide 3-kinase pathway. *Science* 296: 1655-1657, 2002.
- Chang F, Lee JT, Navolanic PM, Steelman LS, Shelton JG, Blalock WL, Franklin RA and McCubrey JA: Involvement of PI3K/Akt pathway in cell cycle progression, apoptosis, and neoplastic transformation: A target for cancer chemotherapy. *Leukemia* 17: 590-603, 2003.
- Nicoletti F, Fagone P, Meroni P, McCubrey J and Bendtzen K: mTOR as a multifunctional therapeutic target in HIV infection. *Drug Discov Today* 16: 715-721, 2011.
- Xu ZZ, Xia ZG, Wang AH, Wang WF, Liu ZY, Chen LY and Li JM: Activation of the PI3K/AKT/mTOR pathway in diffuse large B cell lymphoma: Clinical significance and inhibitory effect of rituximab. *Ann Hematol* 92: 1351-1358, 2013.
- Hans CP, Weisenburger DD, Greiner TC, Gascoyne RD, Delabie J, Ott G, Müller-Hermelink HK, Campo E, Braziel RM, Jaffe ES, *et al*: Confirmation of the molecular classification of diffuse large B-cell lymphoma by immunohistochemistry using a tissue microarray. *Blood* 103: 275-282, 2004.
- Ott G, Ziepert M, Klapper W, Horn H, Szczepanowski M, Bernd HW, Thorns C, Feller AC, Lenze D, Hummel M, *et al*: Immunoblastic morphology but not the immunohistochemical GCB/nonGCB classifier predicts outcome in diffuse large B-cell lymphoma in the RICOVER-60 trial of the DSHNHL. *Blood* 116: 4916-4925, 2010.
- Mahadevan D, Chiorean EG, Harris WB, Von Hoff DD, Stejskal-Barnett A, Qi W, Anthony SP, Younger AE, Rensvold DM, Cordova F, *et al*: Phase I pharmacokinetic and pharmacodynamic study of the pan-PI3K/mTORC vascular targeted pro-drug SF1126 in patients with advanced solid tumours and B-cell malignancies. *Eur J Cancer* 48: 3319-3327, 2012.
- Bendell JC, Rodon J, Burris HA, de Jonge M, Verweij J, Birlle D, Demanse D, De Buck SS, Ru QC, Peters M, *et al*: Phase I, dose-escalation study of BKM120, an oral pan-Class I PI3K inhibitor, in patients with advanced solid tumors. *J Clin Oncol* 30: 282-290, 2012.
- Cheng Y, Zhang Y, Zhang L, Ren X, Huber-Keener KJ, Liu X, Zhou L, Liao J, Keihack H, Yan L, *et al*: MK-2206, a novel allosteric inhibitor of Akt, synergizes with gefitinib against malignant glioma via modulating both autophagy and apoptosis. *Mol Cancer Ther* 11: 154-164, 2012.
- Donia M, Mangano K, Amoroso A, Mazzarino MC, Imbesi R, Castrogiovanni P, Coco M, Meroni P and Nicoletti F: Treatment with rapamycin ameliorates clinical and histological signs of protracted relapsing experimental allergic encephalomyelitis in Dark Agouti rats and induces expansion of peripheral CD4⁺CD25⁺Foxp3⁺ regulatory T cells. *J Autoimmun* 33: 135-140, 2009.
- Bagherpour B, Salehi M, Jafari R, Bagheri A, Kiani-Esfahani A, Edalati M, Kardi MT and Shaygannejad V: Promising effect of rapamycin on multiple sclerosis. *Mult Scler Relat Disord* 26: 40-45, 2018.
- Nguyen QD, Merrill PT, Clark WL, Banker AS, Fardeau C, Franco P, LeHoang P, Ohno S, Rathinam SR, Thurau S, *et al*: Intravitreal sirolimus for noninfectious uveitis: A Phase III sirolimus study assessing double-masked uveitis TReatment (SAKURA). *Ophthalmology* 123: 2413-2423, 2016.
- Stelman LS, Martelli AM, Cocco L, Libra M, Nicoletti F, Abrams SL and McCubrey JA: The therapeutic potential of mTOR inhibitors in breast cancer. *Br J Clin Pharmacol* 82: 1189-1212, 2016.
- Leonardi GC, Falzone L, Salemi R, Zanghi A, Spandidos DA, McCubrey JA, Candido S and Libra M: Cutaneous melanoma: From pathogenesis to therapy (Review). *Int J Oncol* 52: 1071-1080, 2018.

23. Donia M, McCubrey JA, Bendtzen K and Nicoletti F: Potential use of rapamycin in HIV infection. *Br J Clin Pharmacol* 70: 784-793, 2010.
24. Nicoletti F, Lapenta C, Donati S, Spada M, Ranazzi A, Cacopardo B, Mangano K, Belardelli F, Perno C and Aquaro S: Inhibition of human immunodeficiency virus (HIV-1) infection in human peripheral blood leucocytes-SCID reconstituted mice by rapamycin. *Clin Exp Immunol* 155: 28-34, 2009.
25. Caporali S, Alvino E, Lacal PM, Levati L, Giurato G, Memoli D, Caprini E, Antonini Cappellini GC and D'Atri S: Targeting the PI3K/AKT/mTOR pathway overcomes the stimulating effect of dabrafenib on the invasive behavior of melanoma cells with acquired resistance to the BRAF inhibitor. *Int J Oncol* 49: 1164-1174, 2016.
26. Yu Y, Yu X, Ma J, Tong Y and Yao J: Effects of NVP-BE235 on the proliferation, migration, apoptosis and autophagy in HT-29 human colorectal adenocarcinoma cells. *Int J Oncol* 49: 285-293, 2016.
27. Chang Z, Shi G, Jin J, Guo H, Guo X, Luo F, Song Y and Jia X: Dual PI3K/mTOR inhibitor NVP-BE235-induced apoptosis of hepatocellular carcinoma cell lines is enhanced by inhibitors of autophagy. *Int J Mol Med* 31: 1449-1456, 2013.
28. Paplomata E, Zelnak A and O'Regan R: Everolimus: Side effect profile and management of toxicities in breast cancer. *Breast Cancer Res Treat* 140: 453-462, 2013.
29. Lew S and Chamberlain RS: Risk of metabolic complications in patients with solid tumors treated with mTOR inhibitors: Meta-analysis. *Anticancer Res* 36: 1711-1718, 2016.
30. Marcinkowska E, Wallace GR and Brown G: The use of 1 α ,25-dihydroxyvitamin D₃ as an anticancer agent. *Int J Mol Sci* 17: E729, 2016.
31. Holick MF: Vitamin D and bone health. *J Nutr* 126 (Suppl 4): 1159S-1164S, 1996.
32. Abu El Maaty MA and Wölfl S: Vitamin D as a novel regulator of tumor metabolism: Insights on potential mechanisms and implications for anti-cancer therapy. *Int J Mol Sci* 18: E2184, 2017.
33. Barreto SG and Neale RE: Vitamin D and pancreatic cancer. *Cancer Lett* 368: 1-6, 2015.
34. Castronovo C, Castronovo V, Nikkels A and Peulen O: Vitamin D anti-cancer activities: Observations, doubts and certainties. *Rev Med Liege* 70: 495-500, 2015 (In French).
35. Duffy MJ, Murray A, Synnott NC, O'Donovan N and Crown J: Vitamin D analogues: Potential use in cancer treatment. *Crit Rev Oncol Hematol* 112: 190-197, 2017.
36. Li MX, Li LF, Zhang L, Xiao ZG, Shen J, Hu W, Zeng Q and Cho CH: Vitamin D and cancer stem cells in the gastrointestinal tract. *Curr Med Chem* 24: 918-927, 2017.
37. Zhang X, Harbeck N, Jeschke U and Doisneau-Sixou S: Influence of vitamin D signaling on hormone receptor status and HER2 expression in breast cancer. *J Cancer Res Clin Oncol* 143: 1107-1122, 2017.
38. Ahn J, Park S, Zuniga B, Bera A, Song CS and Chatterjee B: Vitamin D in prostate cancer. *Vitam Horm* 100: 321-355, 2016.
39. Lisse TS, Liu T, Irmiler M, Beckers J, Chen H, Adams JS and Hewison M: Gene targeting by the vitamin D response element binding protein reveals a role for vitamin D in osteoblast mTOR signaling. *FASEB J* 25: 937-947, 2011.
40. Jang W, Kim HJ, Li H, Jo KD, Lee MK, Song SH and Yang HO: 1,25-Dihydroxyvitamin D₃ attenuates rotenone-induced neurotoxicity in SH-SY5Y cells through induction of autophagy. *Biochem Biophys Res Commun* 451: 142-147, 2014.
41. Datta Mitra A, Raychaudhuri SP, Abria CJ, Mitra A, Wright R, Ray R and Kundu-Raychaudhuri S: 1 α ,25-Dihydroxyvitamin-D₃-3-bromoacetate regulates AKT/mTOR signaling cascades: A therapeutic agent for psoriasis. *J Invest Dermatol* 133: 1556-1564, 2013.
42. Gröschel C, Tennakoon S and Kállay E: Cytochrome P450 Vitamin D hydroxylases in inflammation and cancer. *Adv Pharmacol* 74: 413-458, 2015.
43. Tannour-Louet M, Lewis SK, Louet JF, Stewart J, Addai JB, Sahin A, Vangapandu HV, Lewis AL, Dittmar K, Pautler RG, *et al*: Increased expression of CYP24A1 correlates with advanced stages of prostate cancer and can cause resistance to vitamin D₃-based therapies. *FASEB J* 28: 364-372, 2014.
44. Sun H, Wang C, Hao M, Sun R, Wang Y, Liu T, Cong X and Liu Y: CYP24A1 is a potential biomarker for the progression and prognosis of human colorectal cancer. *Hum Pathol* 50: 101-108, 2016.
45. Sakaki T, Yasuda K, Kittaka A, Yamamoto K and Chen TC: CYP24A1 as a potential target for cancer therapy. *Anticancer Agents Med Chem* 14: 97-108, 2014.
46. Osanai M and Lee GH: CYP24A1-induced vitamin D insufficiency promotes breast cancer growth. *Oncol Rep* 36: 2755-2762, 2016.
47. Hu N and Zhang H: CYP24A1 depletion facilitates the antitumor effect of vitamin D₃ on thyroid cancer cells. *Exp Ther Med* 16: 2821-2830, 2018.
48. Ng AK, Weiss L and LaCasce AS: Chapter 74 - Hodgkin's Lymphoma. In: *Clinical Radiation Oncology* (3rd Edition). Gunderson LL and Tepper JE (eds). W.B. Saunders, Philadelphia, pp1527-1543, 2012.
49. Koziolowicz P, Grafton G, Kutner A, Curnow SJ, Gordon J and Barnes NM: Novel vitamin D analogues; cytotoxic and anti-proliferative activity against a diffuse large B-cell lymphoma cell line and B-cells from healthy donors. *J Steroid Biochem Mol Biol* 164: 98-105, 2016.
50. Hickish T, Cunningham D, Colston K, Millar BC, Sandle J, Mackay AG, Soukop M and Sloane J: The effect of 1,25-dihydroxyvitamin D₃ on lymphoma cell lines and expression of vitamin D receptor in lymphoma. *Br J Cancer* 68: 668-672, 1993.
51. Klionsky DJ, Abdalla FC, Abeliovich H, Abraham RT, Acevedo-Arozena A, Adeli K, Agholme L, Agnello M, Agostinis P, Aguirre-Ghiso JA, *et al*: Guidelines for the use and interpretation of assays for monitoring autophagy. *Autophagy* 8: 445-544, 2012.
52. Chung I, Karpf AR, Muindi JR, Conroy JM, Nowak NJ, Johnson CS and Trump DL: Epigenetic silencing of CYP24 in tumor-derived endothelial cells contributes to selective growth inhibition by calcitriol. *J Biol Chem* 282: 8704-8714, 2007.
53. Drake MT, Maurer MJ, Link BK, Habermann TM, Ansell SM, Micallef IN, Kelly JL, Macon WR, Nowakowski GS, Inwards DJ, *et al*: Vitamin D insufficiency and prognosis in non-Hodgkin's lymphoma. *J Clin Oncol* 28: 4191-4198, 2010.
54. Ikezoe T, Bandobashi K, Yang Y, Takeuchi S, Sekiguchi N, Sakai S, Koeffler HP and Taguchi H: HIV-1 protease inhibitor ritonavir potentiates the effect of 1,25-dihydroxyvitamin D₃ to induce growth arrest and differentiation of human myeloid leukemia cells via down-regulation of CYP24. *Leuk Res* 30: 1005-1011, 2006.
55. Ly LH, Zhao XY, Holloway L and Feldman D: Liarozole acts synergistically with 1 α ,25-dihydroxyvitamin D₃ to inhibit growth of DU 145 human prostate cancer cells by blocking 24-hydroxylase activity. *Endocrinology* 140: 2071-2076, 1999.
56. Adorini L and Penna G: Control of autoimmune diseases by the vitamin D endocrine system. *Nat Clin Pract Rheumatol* 4: 404-412, 2008.
57. Agmon-Levin N, Theodor E, Segal RM and Shoenfeld Y: Vitamin D in systemic and organ-specific autoimmune diseases. *Clin Rev Allergy Immunol* 45: 256-266, 2013.
58. Young KA, Munroe ME, Guthridge JM, Kamen DL, Niewold TB, Gilkeson GS, Weisman MH, Ishimori ML, Kelly J, Gaffney PM, *et al*: Combined role of vitamin D status and CYP24A1 in the transition to systemic lupus erythematosus. *Ann Rheum Dis* 76: 153-158, 2017.
59. Kleinstern G, Averbuch M, Abu Seir R, Perlman R, Ben Yehuda D and Paltiel O: Presence of autoimmune disease affects not only risk but also survival in patients with B-cell non-Hodgkin lymphoma. *Hematol Oncol* 36: 457-462, 2018.
60. Barcellini W, Rizzardi GP, Borghi MO, Nicoletti F, Fain C, Del Papa N and Meroni PL: In vitro type-1 and type-2 cytokine production in systemic lupus erythematosus: Lack of relationship with clinical disease activity. *Lupus* 5: 139-145, 1996.
61. Narazaki M and Kishimoto T: The two-faced cytokine IL-6 in host defense and diseases. *Int J Mol Sci* 19: E3528, 2018.
62. Dlouhy I, Filella X, Rovira J, Magnano L, Rivas-Delgado A, Baumann T, Martínez-Trillos A, Balagué O, Martínez A, González-Farre B, *et al*: High serum levels of soluble interleukin-2 receptor (sIL2-R), interleukin-6 (IL-6) and tumor necrosis factor alpha (TNF) are associated with adverse clinical features and predict poor outcome in diffuse large B-cell lymphoma. *Leuk Res* 59: 20-25, 2017.
63. Ysmail-Dahlouk L, Nouari W and Aribi M: 1,25-dihydroxyvitamin D₃ down-modulates the production of proinflammatory cytokines and nitric oxide and enhances the phosphorylation of monocyte-expressed STAT6 at the recent-onset type 1 diabetes. *Immunol Lett* 179: 122-130, 2016.
64. Yang M, Xu J, Yu J, Yang B, Gan H, Li S and Li X: Anti-inflammatory effects of 1,25-dihydroxyvitamin D₃ in monocytes cultured in serum from patients with type 2 diabetes mellitus and diabetic nephropathy with uremia via Toll-like receptor 4 and nuclear factor- κ B p65. *Mol Med Rep* 12: 8215-8222, 2015.

65. Lockshin RA and Zakeri Z: Caspase-independent cell deaths. *Curr Opin Cell Biol* 14: 727-733, 2002.
66. Matsui Y, Takagi H, Qu X, Abdellatif M, Sakoda H, Asano T, Levine B and Sadoshima J: Distinct roles of autophagy in the heart during ischemia and reperfusion: Roles of AMP-activated protein kinase and Beclin 1 in mediating autophagy. *Circ Res* 100: 914-922, 2007.
67. Takagi H, Matsui Y, Hirotani S, Sakoda H, Asano T and Sadoshima J: AMPK mediates autophagy during myocardial ischemia in vivo. *Autophagy* 3: 405-407, 2007.
68. Maiuri MC, Tasdemir E, Criollo A, Morselli E, Vicencio JM, Carnuccio R and Kroemer G: Control of autophagy by oncogenes and tumor suppressor genes. *Cell Death Differ* 16: 87-93, 2009.
69. Wullschlegel S, Loewith R and Hall MN: TOR signaling in growth and metabolism. *Cell* 124: 471-484, 2006.
70. Lisse TS and Hewison M: Vitamin D: A new player in the world of mTOR signaling. *Cell Cycle* 10: 1888-1889, 2011.
71. Peponi E, Drakos E, Reyes G, Leventaki V, Rassidakis GZ and Medeiros LJ: Activation of mammalian target of rapamycin signaling promotes cell cycle progression and protects cells from apoptosis in mantle cell lymphoma. *Am J Pathol* 169: 2171-2180, 2006.
72. Rudelius M, Pittaluga S, Nishizuka S, Pham TH, Fend F, Jaffe ES, Quintanilla-Martinez L and Raffeld M: Constitutive activation of Akt contributes to the pathogenesis and survival of mantle cell lymphoma. *Blood* 108: 1668-1676, 2006.
73. Hasselblom S, Hansson U, Olsson M, Torén L, Bergström A, Nilsson-Ehle H and Andersson PO: High immunohistochemical expression of p-AKT predicts inferior survival in patients with diffuse large B-cell lymphoma treated with immunochemotherapy. *Br J Haematol* 149: 560-568, 2010.
74. Maksimovic-Ivanic D, Fagone P, McCubrey J, Bendtzen K, Mijatovic S and Nicoletti F: HIV-protease inhibitors for the treatment of cancer: Repositioning HIV protease inhibitors while developing more potent NO-hybridized derivatives? *Int J Cancer* 140: 1713-1726, 2017.
75. Rothweiler F, Michaelis M, Brauer P, Otte J, Weber K, Fehse B, Doerr HW, Wiese M, Kreuter J, Al-Abed Y, *et al*: Anticancer effects of the nitric oxide-modified saquinavir derivative saquinavir-NO against multidrug-resistant cancer cells. *Neoplasia* 12: 1023-1030, 2010.
76. Maksimovic-Ivanic D, Mojic M, Bulatovic M, Radojkovic M, Kuzmanovic M, Ristic S, Stosic-Grujicic S, Miljkovic D, Cavalli E, Libra M, *et al*: The NO-modified HIV protease inhibitor as a valuable drug for hematological malignancies: Role of p70S6K. *Leuk Res* 39: 1088-1095, 2015.
77. Pearce LR, Alton GR, Richter DT, Kath JC, Lingardo L, Chapman J, Hwang C and Alessi DR: Characterization of PF-4708671, a novel and highly specific inhibitor of p70 ribosomal S6 kinase (S6K1). *Biochem J* 431: 245-255, 2010.
78. Guo LS, Li HX, Li CY, Zhang SY, Chen J, Wang QL, Gao JM, Liang JQ, Gao MT and Wu YJ: Synergistic antitumor activity of vitamin D3 combined with metformin in human breast carcinoma MDA-MB-231 cells involves m-TOR related signaling pathways. *Pharmazie* 70: 117-122, 2015.
79. Yang J, Ikezoe T, Nishioka C, Ni L, Koeffler HP and Yokoyama A: Inhibition of mTORC1 by RAD001 (everolimus) potentiates the effects of 1,25-dihydroxyvitamin D(3) to induce growth arrest and differentiation of AML cells in vitro and in vivo. *Exp Hematol* 38: 666-676, 2010.



This work is licensed under a Creative Commons Attribution-NonCommercial-NoDerivatives 4.0 International (CC BY-NC-ND 4.0) License.